Original Article

ADSCs encapsulated in Gelatin methacrylate substrate promotes the repair of peripheral nerve injury by SIRT6/PGC-1α pathway

Yang Xiang [a, b, 1], Xin Li [c, 1], Yuye Huang [d], Suyue Gao [e], Peng Wei [b], Lijun Wu [f, *], Jun Dong [a, **]

[a] Department of Neurosurgery, The Second Affiliated Hospital of Soochow University, Soochow, China
[b] Department of Plastic Surgery, The First Affiliated Hospital of Ningbo University, Ningbo, China
[c] Jiaxing Shuguang Cosmetic Hospital, Cosmetic Surgery Department, Jiaxing, China
[d] Center for Medical and Engineering Innovation, Central Laboratory, The First Affiliated Hospital of Ningbo University, Ningbo, China
[e] Department of Burns and Wound Repair, The First Affiliated Hospital of Sun Yat-sen University, Guangzhou, China
[f] Department of Plastic and Aesthetic Surgery, the Second Affiliated Hospital of Soochow University, Suzhou, China

ARTICLE INFO

ABSTRACT

Peripheral nerve injury is a prevalent disease but the spontaneous recovery of nerve function is protracted and incomplete. Given the damaging of stem cells and fragile of intra-neural structures in the course of stem cell transplantation, our study tried to investigate whether encapsulating adipose derived mesenchymal stem cells (ADSCs) with GelMA could achieve better repair in peripheral nerve injury. PC-12 cells were cultured on the surface of GelMA encapsulating ADSCs and 3D co-culture system was constructed. CCK-8, Real-Time PCR, ELISA, Immunofluorescent Assay and Western Blot were used to evaluate the functionality of this system. Ultimately, nerve conduit containing the 3D co-culture system was linked between the two ends of an injured nerve. ADSCs encapsulated in 5% GelMA had a better activity than 10% GelMA. Furthermore, the viability of PC-12 cells was also better in this 3D co-culture system than in co-culture system with ADSCs without GelMA. The expression of SIRT6 and PGC-1α in PC-12 cells were prominently promoted, and the entry to nuclear of PGC-1α was more obvious in this 3D co-culture system. After silencing of SIRT6, the protein expression level of PGC-1α was inhibited, and the activity of PC-12 cells was significantly reduced, suggesting that ADSCs encapsulated in GelMA upregulated the expression of SIRT6 to induce the level of PGC-1α protein, thereby achieving an impact on the activity of PC-12 cells. *In vivo*, nerve conduit containing the 3D co-culture system significantly promoted the repair of damaged peripheral nerves. In conclusion, our study demonstrated that 5% GelMA enhanced ADSCs activity, thereby promoting the activity of nerve cells and repair of damaged peripheral nerves by SIRT6/PGC-1α pathway.

© 2024 The Author(s). Published by Elsevier BV on behalf of The Japanese Society for Regenerative Medicine. This is an open access article under the CC BY-NC-ND license (http://creativecommons.org/licenses/by-nc-nd/4.0/).

1. Introduction

Peripheral nerve injury (PNI) is a prevalent clinical condition, commonly attributed to factors such as trauma, infection, tumors, iatrogenic injuries, and other etiologies [1]. In developed nations, the incidence of PNI stands at 13—23 per 100,000 individuals every year [2]. While self-recovery is possible following peripheral nervous system injury, the dependence of axon extension on the synthesis and transport of intracellular matrix often result in a protracted and incomplete recuperation process [3]. The general consensus in clinical practice is that surgery typically yields superior outcomes in terms of peripheral nerve recovery. When the peripheral nerve defect is less than 5 mm, an "end-to-end" nerve suture can be used, and when the defect is larger than 5 mm, autogenous nerve transplantation is considered as the "gold standard" [4,5]. However, autogenous nerve transplantation also has some defects, such as secondary nerve injury in donor area, limited donor area, mismatch of nerve size [2,6].

* Corresponding author. Department of Plastic and Aesthetic Surgery, the Second Affiliated Hospital of Soochow University, Suzhou 215004, China.
** Corresponding author. Department of Neurosurgery, The Second Affiliated Hospital of Soochow University, Suzhou 215004, China.
E-mail addresses: ljwu1986@163.com (L. Wu), dongjun@suda.edu.cn (J. Dong).
Peer review under responsibility of the Japanese Society for Regenerative Medicine.
[1] These authors contribute equally to this study.

The tissue engineering tubular structure, responsible for connecting the proximal and distal nerve stump, is referred to as nerve conduit, which comprises of natural or synthetic polymers and encompasses both physical and biological factors that facilitate cell regeneration guidance. The nerve conduit avoids the defects of donor site dysfunction, donor site limitation, donor area secondary injury in nerve transplantation and direct nerve suture [7]. The ideal nerve conduit should encompass the following attributes: providing a place for growth factor aggregation and Schwann cell growth, as well as guiding nerve extension from proximal towards the distal region [8]. Seed cells play a pivotal role in tissue engineering nerve conduits due to their capacity for proliferation and differentiation into specific tissues for defect repair [9]. Ideal cells should include the following characteristics: wide source, good security, no ethical restrictions, no immune rejection [10,11]. Schwann cells are important cells in peripheral nerve regeneration, and they are glial cells arranged along axons. Schwann cells can promote nerve regeneration by up-regulating axonotrophic cellular adhesion molecules and secreting neurotrophic factors such as NGF, GDNF and BDNF(12). However, Schwann cells have high requirements for *in vitro* culture and slow growth, so it is not easy to further popularize Schwann cells in clinic [13] in the future. Secondly, obtaining a sufficient number of autologous Schwann cells will also cause morbidity of the donor site. Finally, the collection of autologous Schwann cells in emergency trauma cases can lead to delays in nerve repair. Consequently, there arises a necessity for an alternative cellular entity possessing comparable regenerative properties to Schwann cells while minimizing donor site damage and ensuring enhanced availability [12].

Mesenchymal stem cells (MSCs) have attracted much attention in the field of regenerative medicine because of their great potential to differentiate into bone, cartilage, muscle, fat and tendons [14,15]. Additionally, the mechanism that MSCs induce neural regeneration has been confirmed [16], and studies suggest that MSCs can differentiate into Schwann-like cells [17,18]. Therefore, later studies directly applied mesenchymal stem cells to replace Schwann cells in peripheral nerve injury and achieved good therapeutic results. There are abundant sources of MSCs, among them, adipose tissue-derived mesenchymal stem cells (ADSCs) have been widely used in clinical and research work because of their features: rich content, easy to obtain, easy to proliferate, strong angiogenic function and less ethical restrictions. Studies have shown that ADSCs have strong electrodynamic characteristics, which make them have better anti-hypoxia and anti-oxidative stress ability [19]. ADSCs and endogenous stem cells collaborate to produce adventitia-like structures for axonal injury repair by releasing numerous growth factors. Recent research indicates that ADSCs possess a stronger ability than endogenous stem cells in inducing motor neuron proliferation and restore neural evoked potentials [20].

Gelatin methacryloyl (GelMA) is produced via the reaction of gelatin and methyacrylic anhydride, and due to their suitable biological properties and physical characteristics, GelMA has found widespread applications in biomedical areas [21]. It's widely used as scaffolds in tissue engineering because of supporting cell attachment and growth of GelMA [22]. Recent study had found that umbilical cord Mesenchymal stem cells (UC-MSCs) exhibited high cellular activity when attached to GelMA [23]. Another study established 3D co-culture model of Schwann cells and neural cells in GelMA, which proved that both Schwann cells and neural cells grew well, and neural cells in 3D co-culture group had a higher cell proliferation rate and axon extension than 2D co-culture group [24]. However, the effect of GelMA loaded ADSCs in nerve regeneration remains unknown and necessitating further elucidation of the 3D co-culture model involving ADSCs interactions with neuron cells need to further confirmed.

Sirtuins are a highly conserved family of nicotinamide adenine dinucleotides (NAD) + dependent enzymes that serves as central regulators of lower biological lifespan [25,26]. There are seven species of sirtuins (SIRT1-7) in mammals [27,28], which have a wide range of cellular functions, including energy metabolism, cellular stress resistance, genomic stability, aging and tumorigenesis [29]. In the SIRT family, SIRT6 has been reported to be involved in transcriptional regulation, genomic stability and lifespan of many cells [30,31]. The role of SIRT6 in peripheral nerve regeneration has also been reported. It has been reported that the inhibition of SIRT6 can inhibit the migration, phagocytosis and M2 polarization of macrophage, and finally delay the recovery of peripheral nerve [32]. The peroxisome proliferator-activated receptorγcoactivator-1 (PGC -1) family includes PGC -1α, PGC -1β and PGC-1 related coactivator, which plays a key role in regulating mitochondrial function and energy homeostasis. In the nervous system, PGC-1α is a group involved in neuronal metabolism, neurotransmission and morphology, and plays a key role in transcription and excitability of excitatory neurons in the neocortex and hippocampus [33]. However, it is unclear that whether ADSCs promote peripheral nerve regeneration through SIRT6 and PGC-1α pathway in a 3D co-culture model.

In this study, we implemented a co-culture system involving ADSCs and rat pheochromocytoma (PC-12) cells on a gelatin methacrylate (GelMA) scaffold to investigate the impact of GelMA-encapsulated ADSCs secretions on PC-12 cells.

2. Materials and methods

2.1. Synthesis of GelMA

Gelatin obtained from porcine skin tissue (250 bloom, Type B), and methacrylic anhydride (MA) was purchased from Aladdin Industrial (Shanghai, China). PDMS was purchased from Sylgard (Midland, MI, USA). The photoinitiator, lithium phenyl-2,4,6- trimenthylbenzoyphosphinate (LAP), was purchased from Engineering for Life (Suzhou, China). Gelatin was dissolved in a buffer solution containing Na_2CO_3 and $NaHCO_3$ at 50 °C under continuous stirring for 3 h until fully dissolved. Next, various volumes (0.025/1 and 0.05/1) of MA were dropped into the gelatin solution to synthesize GelMA with various degrees of methacryloyl substitution (DMS, 30% and 50%, respectively). After reacting in the dark for 3 h, samples were diluted with 5-fold deionized water and dialyzed for 3 day at room temperature with water changes three times per day. Finally, GelMA solutions were frozen at −80 °C, lyophilized for three days, and stored at −20 °C for further use. A scanning electron microscope (SEM, TM-100, Hitachi, Tokyo, Japan) was used to observe the pore structures of GelMA hydrogels with different DMS and concentrations.

2.2. Extraction of ADSCs from rats

Under aseptic condition, adipose tissue was extracted from the groin subcutaneously or around the epididymis of rats, and washed twice with PBS. Microtweezer was used to removed blood vessels and connective tissue visible to the naked eye, and ophthalmic scissor was utilized to cut the adipose tissue into small pieces, about the size of 1 mm³. The chopped adipose tissue was digested with 0.2% I collagenase of the same volume and then digested in a water bath at 37 °C for 1.5 h, during which the adipose tissue was shaken intermittently to make it fully digested. The same volume of complete culture medium (90% DMEM-F12 (Gibco, Invitrogen, USA) +10% fetal bovine serum (YEASEN, Shanghai, China) + 1% double antibody (Gibco, Invitrogen, USA)) terminated 0.25% trypsin-EDTA (1 mM, Gibco, Big Cabin, OK, USA) digestion, 200

mesh sieve filtration, 1000 r/min centrifugation 5 min, discarding the supernatant, adding PBS resuspension cells and centrifuging again. The cells were resuscitated in complete culture medium, inoculated in 25 mm^2 culture flask and cultured at 37 °C in 5% CO_2 incubator for 48 h. Morphology of ADSCs was observed under an inverted microscope after changing the liquid every 2 days.

2.3. Passage of ADSCs

When the primary cells grow to 80%–90% in the culture bottle, the passage culture was carried out. The cells were digested by 0.25% trypsin-EDTA (1 mM, Gibco, Big Cabin, OK, USA) after discarding the culture medium. The cells became round and brightened under the inverted microscope, and the digestion was terminated immediately with the same volume of complete culture medium. The single cell suspension was made by gently blowing the bottom of bottle with a straw and centrifuged by 1000 r/min. The supernatant was discarded and the cells were re-suspended in the complete culture medium. According to the proportion of 1:2, the cells were inoculated in the new culture flask and cultured in the 5% CO_2 incubator at 37 °C. The liquid was replaced every 2 days until the cell grows to 80%–90% at the bottle. Repeat the above operation and pass it on.

2.4. Adipogenic induction

The third-generation adipose stem cells of logarithmic growth were inoculated into 6-well plate according to 2×10^4 cells/cm^2, and 2 ml complete culture medium was added to each well. The cells were divided into observation and control group. When the degree of cell fusion reached 100% or over-fusion, adipogenic induction solution was added in the observation group, 2 ml/hole, medium was replaced every 3 days and the morphological changes of cells were observed under inverted microscope. The control group was cultured with complete culture medium which was changed every 3 days. After 2 weeks of induction, oil red O staining was performed. The plate was washed by PBS and fixed with 4% neutral formaldehyde. Oil red O solution (Beyotime, Shanghai, China) was added, and 30 min was dyed. The oil red O dye was removed and the excess dye was rinsed with PBS. The cells were observed under an inverted microscope after staining (Fig. 1A).

2.5. Osteogenic induction

The third generation of ADSCs were inoculated in 6-well plates and divided into observation and control group. In the observation group, when the degree of cell fusion reached to 60%–70%, osteogenic induction solution was added 2 ml per well. The fluid was changed once every 3 days. When a large number of calcium nodules occur during the osteogenesis process, medium was changed every 2 days in order to prevent the loss of osteoblasts. The control group was cultured with complete culture medium and the medium was changed every 3 days. After 2 weeks of induction, 2 ml 4% neutral formaldehyde solution was added, and the 1 ml/hole was fixed for 30 min. PBS washed the cells and alizarin red solution (Beyotime, Shanghai, China) was added. The staining effect was observed under microscope after staining 5 min (Fig. 1B).

2.6. ADSCs encapsulation in GelMA

Two concentrations (5% and 10%) of GelMA precursor solution were prepared by dissolving in a fully supplemented cell culture medium carrying 0.5% (w/v) with LAP as a photoinitiator. ADSCs were trypsinized by 0.25% Trypsin-EDTA (1 mM, Gibco, Big Cabin, OK, USA) when the cell reached 70–80% confluency and were

resuspended in GelMA solution with a final cell density of 1×10^6 cells/ml. The cell suspension was immediately crosslinked with ultraviolet light (405 nm, 10 W/cm^2) at a distance of 1 cm for 1 min, resulting in a cylinder GelMA encapsulated with ADSCs. These irradiation parameters have been optimized and shown to maximize the crosslinking of monomers chains.

2.7. 3D co-culture system construction

The ADSC-laden gels were added to the lower chamber of the 24-well plate and PC-12 cells were placed in the Upper chamber, which was then placed at 37 °C, 5% CO2, and 90% humidity for 24 h. As was shown in Fig. 1C, the co-culture model was performed by seeding PC-12 cells on the surface of ADSCs encapsulated in GelMA referred to previous literature [24]. ADSCs encapsulated in GelMA were transferred to culture plates, PC-12 cell suspension (2×10^5 cells/ml) was added to the well and dropped freely on the GelMA surface. PC-12 cells seeded on the GelMA without ADSCs were also prepared as a control group. The follow-up experiments *in vitro* were performed in this system.

2.8. Cellular proliferation analysis

CCK-8 assays (Beyotime, Shanghai, China) were carried out on days 0, 1, 3, 5, and 7 to investigate the proliferation of the ADSCs with different concentrations of GelMA. At every point of time, cell-laden samples (n > 3) were transferred into a new tissue culture plate to avoid the influence of cells growing on the bottom of the plate that dropped out from GelMA. CCK-8 assay was performed according to the manufacturer's protocol, where CCK-8 working solution was prepared with fully supplemented media and incubated with samples for 2 h. The CCK-8 solution was then transferred to a 96-well plate for fluorescence reading at 450 nm. The cellular proliferation rate of each time point was evaluated by normalizing to the day 0 absorbance. The cellular proliferation for the co-culture system was also evaluated using the same protocol mentioned above.

2.9. Real-time PCR

The RNAs of ADSCs cultured in 3D and 5% GelMA were harvested using TRIzol (Beyotime, Shanghai, China), further insolated using chloroform (Guoyao, Shanghai, China), and washed with isopropanol (Guoyao, Shanghai, China) once and 75% ethanol (Guoyao, Shanghai, China) twice. The extracted RNA was finally dissolved in RNase-free water, and the concentration was measured by Nanodrop (Thermo Scientific, Waltham, MA, USA). Complementary DNA (cDNA) was synthesized using the FastKing gDNA Dispelling RT SuperMix kit (YEASEN, Shanghai, China). Relative gene expression analysis was evaluated using real-time PCR (Roche, Basel, Switzerland). Power SYBR Green PCR Master Mix (YEASEN, Shanghai, China) was mixed with 50 ng cDNA and specific primers (Table 1, Sangon Biotech, Shanghai, China) in a total volume of 10 μl.

2.10. ELISA assay

The secretion of β-NGF (Sangon Biotech, Shanghai, China), BDNF (Sangon Biotech, Shanghai, China), and GDNF (Sangon Biotech, Shanghai, China) of ADSCs were measured using an ELISA assay based on the manufacturer's protocol. The supernatant of ADSCs laden GelMA or ADSCs (5% and 10%) at day 1, 3, 5, and 7 was collected and analyzed by a microplate reader (Bio-Rad, San Francisco, USA).
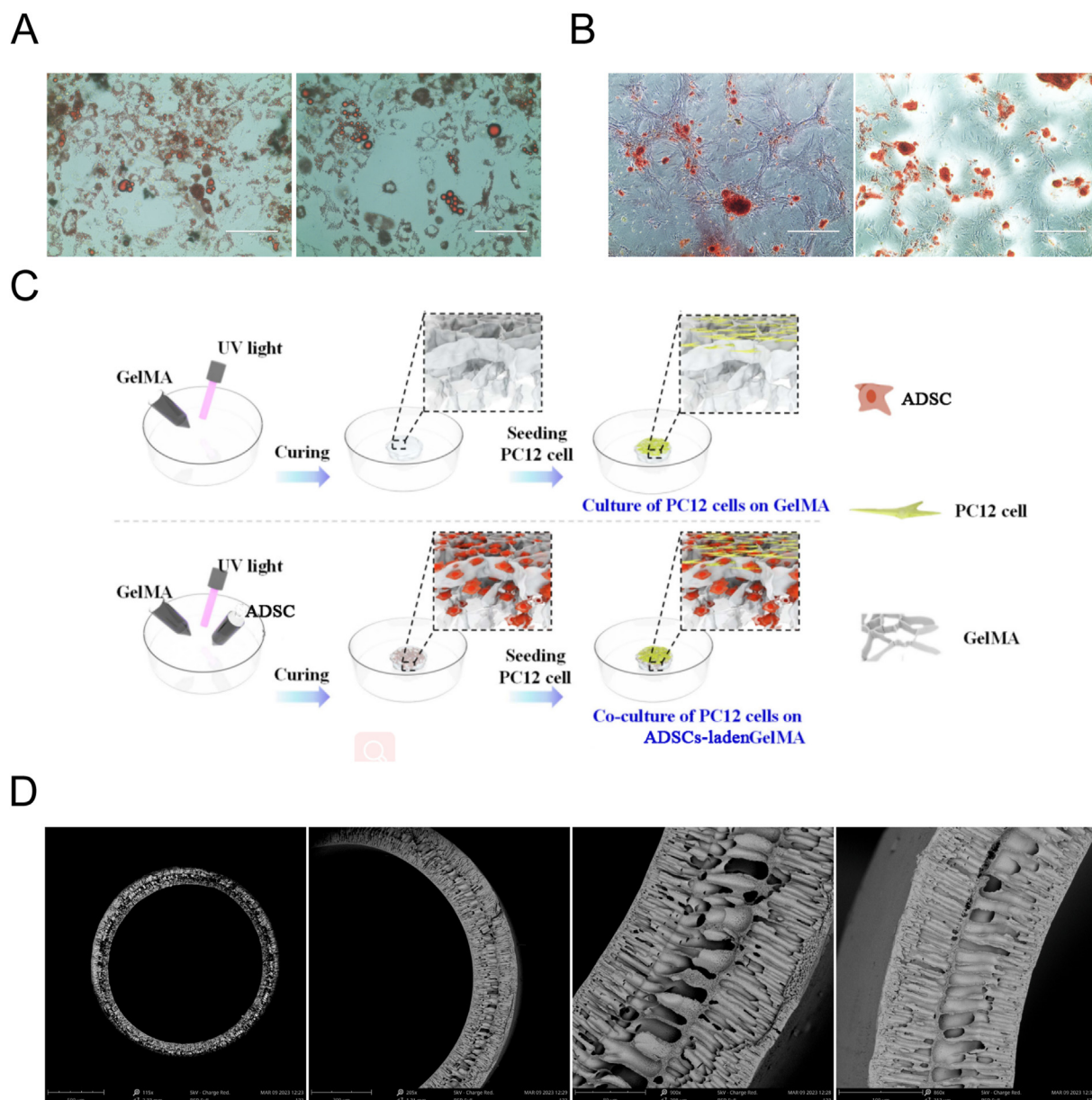
Fig. 1. (A) Adipogenic differentiation of ADSCs was confirmed. (B) Osteogenic differentiation of ADSCs was confirmed. (C) The schematic diagram of co-culture system. (D) The schematic diagram of PLGA catheters.

2.11. Immunofluorescent Assay

The immunofluorescence staining was used to evaluate the protein expression of PC-12 cells. Samples were fixed in 4% para-formaldehyde (PFA, Solarbio, Beijing, China) for 2 h, washed with PBS three times, permeabilized with 0.5% Triton X-100 (Beyotime, Shanghai, China) for 15 min, and blocked with blocking buffer (3% BSA) for 2 h at room temperature. Primary antibodies including βIII tubulin (Abcam, Cambridge, UK, 1:200), PGC-1α (Proteintech, USA, 1:100) and SIRT6 (Proteintech, USA, 1:200) were used for PC-12. After incubation at 4 °C overnight, samples were washed with PBS and stained with secondary antibodies including Cy3-conjugated AffiniPure goat anti-rabbit IgG (H + L) (Jackson ImmunoResearch, USA, 1:500) and Alexa Fluor 488-conjugated AffiniPure goat anti-mouse IgG (H + L) (Jackson ImmunoResearch, USA, 1:500) for 1 h at room temperature. In addition, cell nuclei were stained with DAPI (Beyotime, Shanghai, China), and samples were washed with PBS

three times before imaging by an inverted phase-contrast fluores-cence microscope (Olympus BX51, Japan).

2.12. Western Blot

Total cellular proteins were extracted by lysing cells with RIPA lysate containing PMSF (Beyotime, Shanghai, China). The protein

Table 1
Primers used for qPCR.

Gene	Forward 5′-3′	Reverse 5′-3′
SIRT6	GCCCTCTCCTCATTGCA	AGCCTTGGGTGCTACTGG
PGC-1α	ATCCTCTTCAAGATCCTGTTACT	CGTGCTCATTGGCTTCATAG
NGF	GGACGCAGCTTTCTATCCTGG	CCCTCTGGGACATTGCTATCTG
BDNF	TCATACTTCGGTTGCATGAAGG	AGACCTCTCGAACCTGCCC
GDNF	CTGACTTGGGTTTGGGCTAC	CCTGGCCTACCTTGTCACTT
GAPDH	AACAGGAGGTCCCTACTCCC	GCCATTTTGCGGTGGAAATG

concentration was determined by BCA protein quantitative kit (Beyotime, Shanghai, China). The protein samples of each group were separated by SDS-PAGE and then transferred to 230 mA constant current ice for 90 min. The PVDF membrane was sealed at room temperature for 1 h in 50 g/L skim milk sealing solution. After blocked by skim milk (5%) for 1 h, membranes were incubated with primary antibodies, including anti-SIRT6 (1:1000, Proteintech, USA), antiPGC1-α (1:1000, Proteintech, USA). Then they were incubated with corresponding secondary antibodies for 1 h at room temperature. After that, blot signals were photographed by enhanced chemiluminescence (ECL) kit (Millipore).

2.13. Transfection

SIRT6 was silenced in PC-12 cells, and PC-12 cells transfected with si-SIRT6 were subsequently co-cultured with ADSCs coated with 5% GeIMA. The Sirt6-specific siRNA target sequences according to previous study [34] were as follows: sense 5′-GUGCAUCU-CAAUGGUUCCUTT-3′, and antisense 5′-AGGAACCAUUGAGAUGC ACTT-3′. Transfected PC-12 cells were co-cultured with ADSCs encapsulated in 5% GeIMA.

2.14. Preparation of nerve conduit

An appropriate amount of PLGA and DMSO solvent were mixed, and the concentration suitable for the preparation of the catheter mixed solution required for this experiment was prepared, the mixed solution with PLGA mass fraction of 17% was used for the preparation of smooth catheters, and the mixed solution with PLGA mass fraction of 16% was used for the preparation of grooved conduit. The mixed solution was stirred until PLGA and DMSO were mixed evenly, and the foam in the mixed solution was removed by standing for 4 h, and the final uniform solution with light yellow color was used as the spinning stock solution for the preparation of the nerve catheter required for this experiment. Deionized water is used for the spinning core solution.

The equipment used to prepare the catheter by dry jet wet spinning in this experiment included: two Harvard syringe pumps, two syringes, a custom spinneret, a spinning stock solution, and a spinning core solution. Two Harvard syringe pumps are used to propel the syringe containing the material for the preparation of the nerve catheter, which is filled with the spinning stock solution and the spinning core solution that required for the preparation of the nerve catheter. By pushing the needle, the spinning stock solution and spinning core solution are pushed into a custom-made spinneret with two separate channels, each with an outlet and an inlet. The spinning core liquid flows out of the inner outlet of the spinneret, while the spinning stock solution flows out of the outer outlet. After the spinning core liquid and the spinning stock solution flow out of the outlet, they first enter the air segment to integrate with each other, and then the spinning stock solution is separated to obtain a hollow nerve catheter with a microporous structure after polymer curing in the stock solution. The entire falling process of the catheter is done in a free fall method, so that no additional force is applied to the catheter during the falling process. Finally, the catheter enters the coagulation bath and is finally formed. The resulting nerve catheter also needs to be soaked in water for at least 24 h to remove residual DMSO solvent. After that, the nerve catheter can be cut into small pieces and preserved in water for further experiments (Fig. 1D).

2.15. Construction of animal models

Male SD rats were randomly divided into 4 groups: group A: autologous nerve transplantation group, group B: PLGA catheter group, group C: PLGA catheter + 5% GeIMA group, group D: PLGA catheter + 5%GeIMA encapsulating ADSCs group, each group contained 6 rats. SD rats are anesthetized by propofol. The right sciatic nerve of each SD rat was surgically dissected, after which the sciatic nerve was excised to a length of 10 mm of the defect as a model for peripheral nerve injury. In the autologous transplant group of group A, the resected nerve tissue of SD rats was reversed by 180° and then bridged. In group B, the two nerve cuffs of SD rats were bridged and sutured by a nerve catheter, the length of the nerve catheter was 12 mm, and the nerve cuffs on both sides were placed in the catheter about 1 mm, so that the distance between the nerve cuffs inside the hollow tube was 10 mm. The nerve catheter and epineurium were sutured under the microscope with a 9-0 gauge suture. In group C, the broken end in the nerve of SD rats were bridged and sutured by a PLGA catheter containing 5% GelMA in the tube. For group D, the broken end in the nerve of SD rats was bridged and sutured by a PLGA catheter which added GelMA encapsulating ADSCs. After bridging the nerve defect, the tissues of SD rats were sutured using a 4-0 suture. Rats after surgery were housed in a constant temperature environment of 25 °C and a 12-h solar cycle environment (Fig. 6A, B and C).

2.16. Statistical analysis

Data were presented as the mean $\pm$ SD, and statistical analyses were performed using SPSS 20.0 (SPSS, Chicago, IL, USA). The student's test was used to calculate the differences between two groups. One-way analysis of variance (ANOVA) was used for comparison between groups, followed by Tukey multiple comparisons. All p-values were two-sided, and ***$p < 0.001$, **$p < 0.01$, *$p < 0.05$ was considered to be statistically significant. All experiments were performed at least three times.

3. Result

3.1. 5% GeIMA was better than 10% GeIMA in promoting ADSCs activity

Activity of ADSCs was measured using CCK-8 and the results showed that ADSCs encapsulated in 5% GeIMA were more active than in 10% GeIMA, and the results became more pronounced from day 3 onwards (Fig. 2A). The protein levels of BDNF, GDNF, and β-NGF in 5% GeIMA and 10% GeIMA were detected by ELISA. The protein levels of BDNF, GDNF, and β-NGF in ADSCs encapsulated with 5% GeIMA were higher than those encapsulated with 10% GeIMA and became more pronounced after day 5 (Fig. 2B–D). It could be concluded that ADSCs encapsulated in 5% GeIMA had more activity than in 10% GeIMA.

3.2. ADSCs encapsulated by 5% GeIMA significantly promoted the activity of PC-12 cells

For verifying the effects of ADSCs encapsulated in GeIMA on PC-12 cells, we established a 3D co-culture model (Fig. 1C). And we compared the experimental results of PC-12 cells alone culture, PC-12 cells and ADSCs co-culture (PC-12 cells + ADSCs), PC-12 cells and 5% GeIMA co-culture (PC-12 cells + 5% GeIMA), PC-12 cells and ADSCs encapsulated in 5% GeIMA co-culture (PC-12 cells + ADSCs + 5% GeIMA). The mRNA expression levels of BDNF, GDNF and β-NGF in the ADSCs of the four groups were detected by Realtime-PCR. The results showed that the mRNA expression levels of BDNF, GDNF and β-NGF were the highest when ADSCs encapsulated in 5% GeIMA were co-cultured with PC-12 cells, followed by PC-12 cells + ADSCs, PC-12 cells + 5% GeIMA, and PC-12 cells cultured alone (Fig. 3A–C).
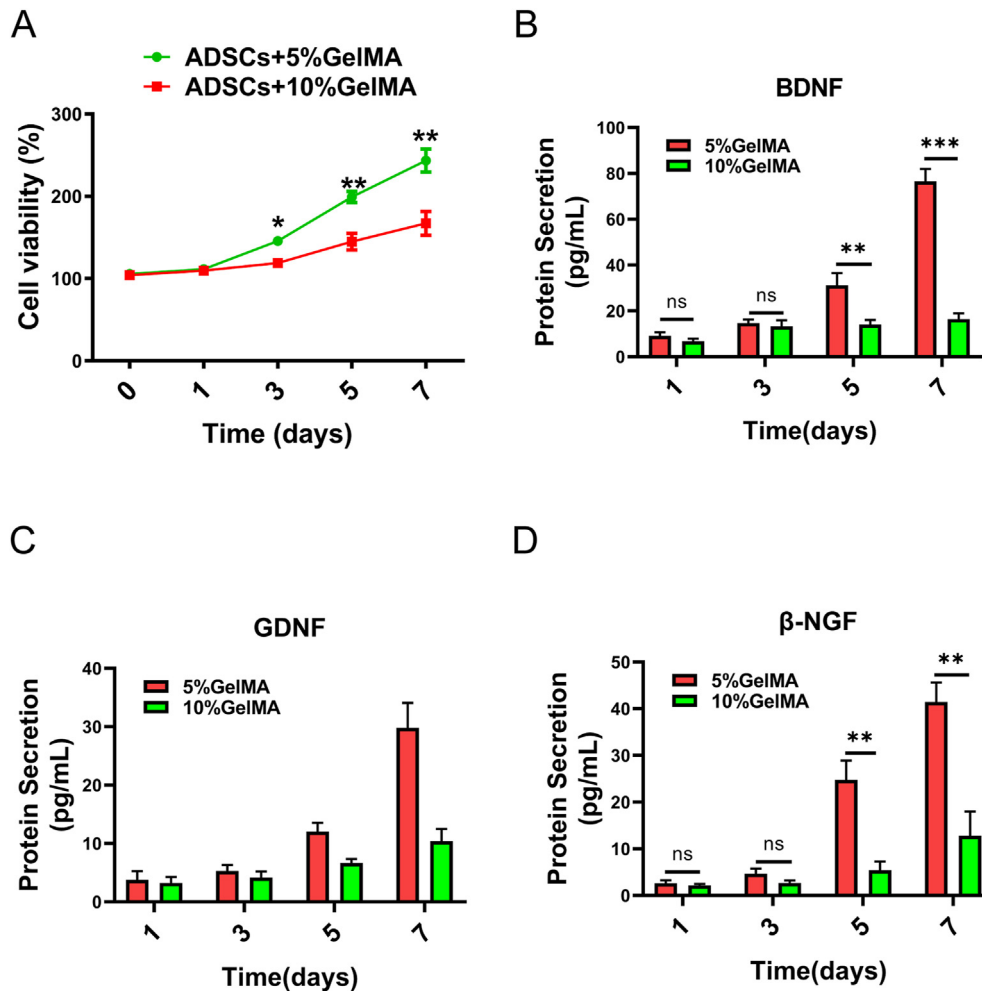
Fig. 2. 5% GelMA significantly promoted ADSC activity more than 10% GelMA. (A) CCK-8 was used to detect ADSC activity. (B) The level of BDNF protein in ADSC medium was detected by ELISA. (C) ELISA was used to detect the level of GDNF protein in ADSCs medium. (D) ELISA was used to detect the protein level of β-NGF in ADSCs medium. ***p < 0.001, **p < 0.01, *p < 0.05 (n = 5).

Next, we used ELISA to measure the protein levels of BDNF, GDNF, and β-NGF in the co-culture system, and found that the protein levels of PC-12 cells + ADSCs encapsulated in 5% GelMA were highest, followed by PC-12 cells + ADSCs. This was followed by PC-12 cells + 5% GelMA and PC-12 cells with the lowest protein level (Fig. 3D−F).

PC-12 cell activity in the four control groups were detected with CCK-8. It can be seen that the activity of PC-12 cells in the four control groups was sorted from high to low: PC-12 cells + ADSCs + 5% GelMA, PC-12 cells + ADSCs, PC-12 cells + 5% GelMA, and PC-12 cells separately (Fig. 3G).

Immunofluorescence assay was performed on PC-12 cells, and the levels of βIII tubulin (green) and DAPI (blue) in PC-12 cells were observed under four conditions: PC-12 cells, PC-12 cells + ADSCs, PC-12 cells + 5% GelMA, and PC-12 cells + 5% GelMA + ADSCs. The results indicated that PC-12 cells in 5% GelMA encapsulating ADSCs co-culture system were better differentiated. The levels of βIII tubulin in the PC-cells were significantly increased after ADSCs co-culture with PC-12 cells, and the secretion of βIII tubulin was further promoted by 5% GelMA encapsulating ADSCs co-culture, while βIII tubulin in the PC-12 cells after co-culture with 5% GelMA did not change significantly. At the same time, ADSCs encapsulated in 5% GelMA promoted PC-12 cells differentiation (Fig. 3G).

3.3. ADSCs encapsulated in 5% GelMA significantly promoted the level of SIRT6/PGC-1α pathway

Western blot assay was performed on PC-12 cells (Fig. 4A) to detect the expression of SIRT6 and PGC-1α, and the expression of the protein was represented by histograms. The results showed that the expression of SIRT6 was the highest in PC-12 cells co-cultured with 5% GelMA-encapsulating ADSCs, followed by co-culture with ADSCs cells, while the expression of SIRT6 was basically the same in 5% GelMA and PC-12 cells alone culture (Fig. 4B). Observing the histogram of PGC-1α expression, it could be seen that the protein expression from high to low when PC-12 cells were co-cultured with 5% GelMA encapsulating ADSCs, ADSCs, 5% GelMA and PC-12 cells alone (Fig. 4C).

Following, we used Rt-PCR to detect SIRT6 and PGC-1α mRNA expression in PC-12 cells. We found that there was no significant change in PGC-1α mRNA expression, while the protein expression of PGC-1α was quite different, suggesting that SIRT6 might regulate PGC-1α protein levels rather than mRNA (Fig. 4D and E). Immunofluorescence staining showed that 5% GelMA-encapsulating ADSCs significantly facilitated PGC-1α nucleation (Fig. 4F).
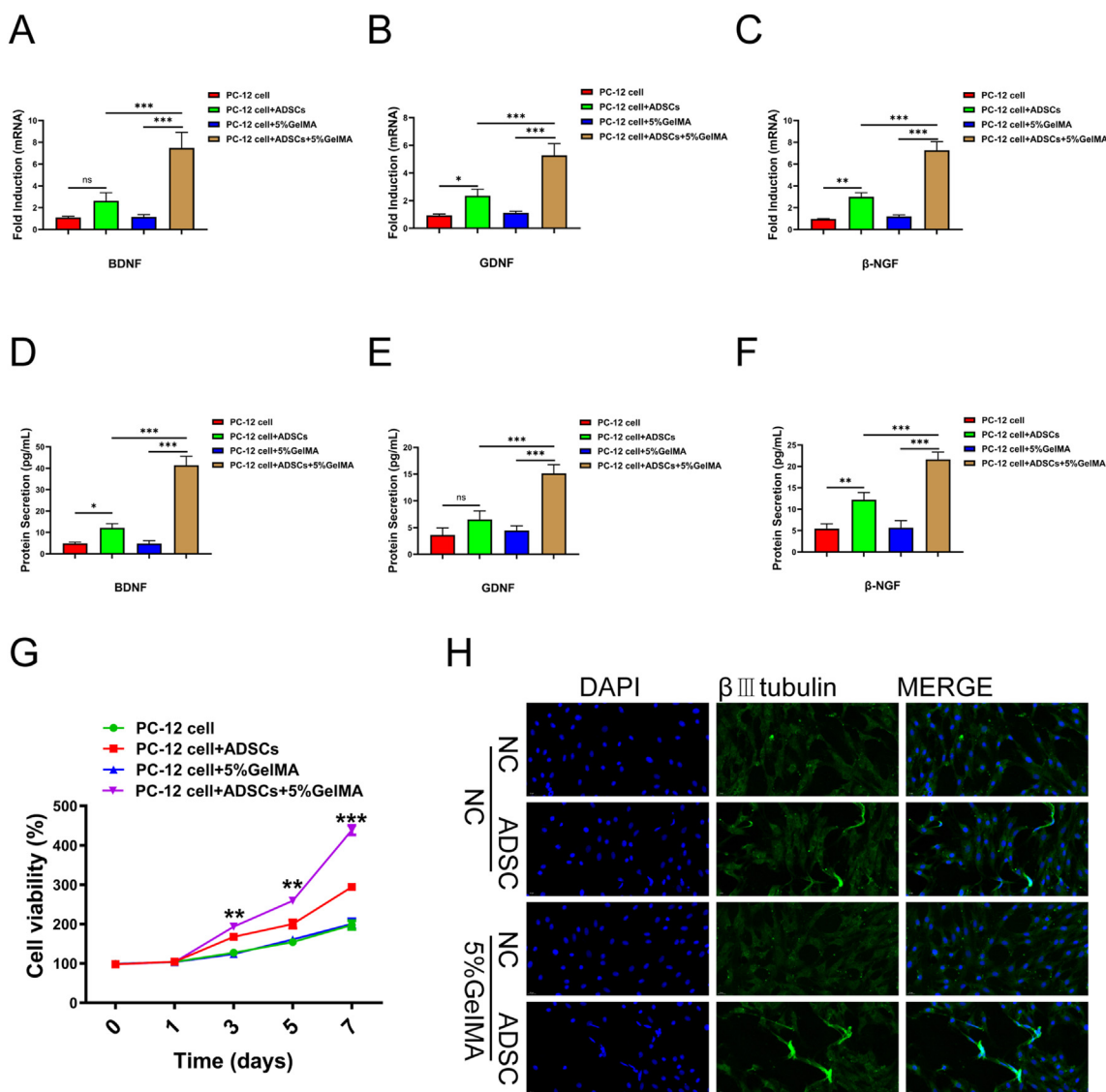
Fig. 3. ADSCs encapsulated in 5% GelMA significantly promoted PC-12 activity. (A–C) Realtime-PCR was used to detect the mRNA expression level of BDNF, GDNF and β-NGF in the ADSCs of co-culture system. (D–F) ELISA was used to detect the protein level of BDNF, GDNF and β-NGF in the co-culture system. (G) CCK-8 detected the activities of PC-12 cells. (H) Immunofluorescence assay results of βIII tubulin and DAPI in PC-12 cells.

3.4. After silencing of SIRT6 in PC-12 cells, the level of PC-12 differentiation was inhibited

SIRT6 was silenced by small interfering RNA to SIRT6 (si-SIRT6) in PC-12 cells, and subsequently PC-12 cells transfected with si-SIRT6 were co-cultured with ADSCs encapsulated in 5% GelMA. Realtime-PCR was used to detect the mRNA expression of SIRT6 and PGC-1α in PC-12 cells. The results showed that mRNA expression level of SIRT6 decreased significantly after transfection of PC-12 cells with si-SIRT6, while the mRNA expression level of PGC-1α did not change significantly (Fig. 5A). Then, Western blot assay was performed to detect the protein expression levels of SIRT6 and PGC-1α. It could be seen that silencing SIRT6 significantly inhibited the protein expression level of PGC-1α, suggesting that SIRT6 promoted the differentiation of PC-12 cells by regulating the protein level of PGC-1α (Fig. 5B and C). CCK-8 assay results showed a significant decrease in PC-12 activity after silencing of SIRT6 (Fig. 5D). Immunofluorescence was performed on PC-12 cells, and the results suggest that silencing of SIRT6 inhibits PC-12 cell differentiation

(Fig. 5E). These results suggested that ADSCs encapsulated in 5% GelMA promoted the differentiation of PC-12 cells by SIRT6/PGC-1α pathway.

3.5. PLGA catheters filled with GelMA-encapsulating ADSCs significantly promoted the repair of peripheral nerve injury

Subsequently, after Poly (lactic-co-glycolic acid) (PLGA) catheters filled with GelMA-encapsulating ADSCs (PLGA + GelMA + ADSCs) were transplanted into the middle of the severed nerve (Fig. 6A, B, C). The diagram of was shown in Fig. 7A. Immunohistochemistry and HE experiment were performed to observe morphology of nerves and protein expression. The growth of nerves was promoted in PLGA + GelMA-encapsulating ADSCs (Fig. 7B). NF200 and S100 staining results suggested that the nerve fibers in the PLGA + GelMA-encapsulating ADSCs were superior to those in the PLGA catheter alone (Fig. 7C and D). The expression of nerve number, NF200 and S100 in the PLGA catheter + GelMA-encapsulating ADSCs were significantly better than those in the PLGA
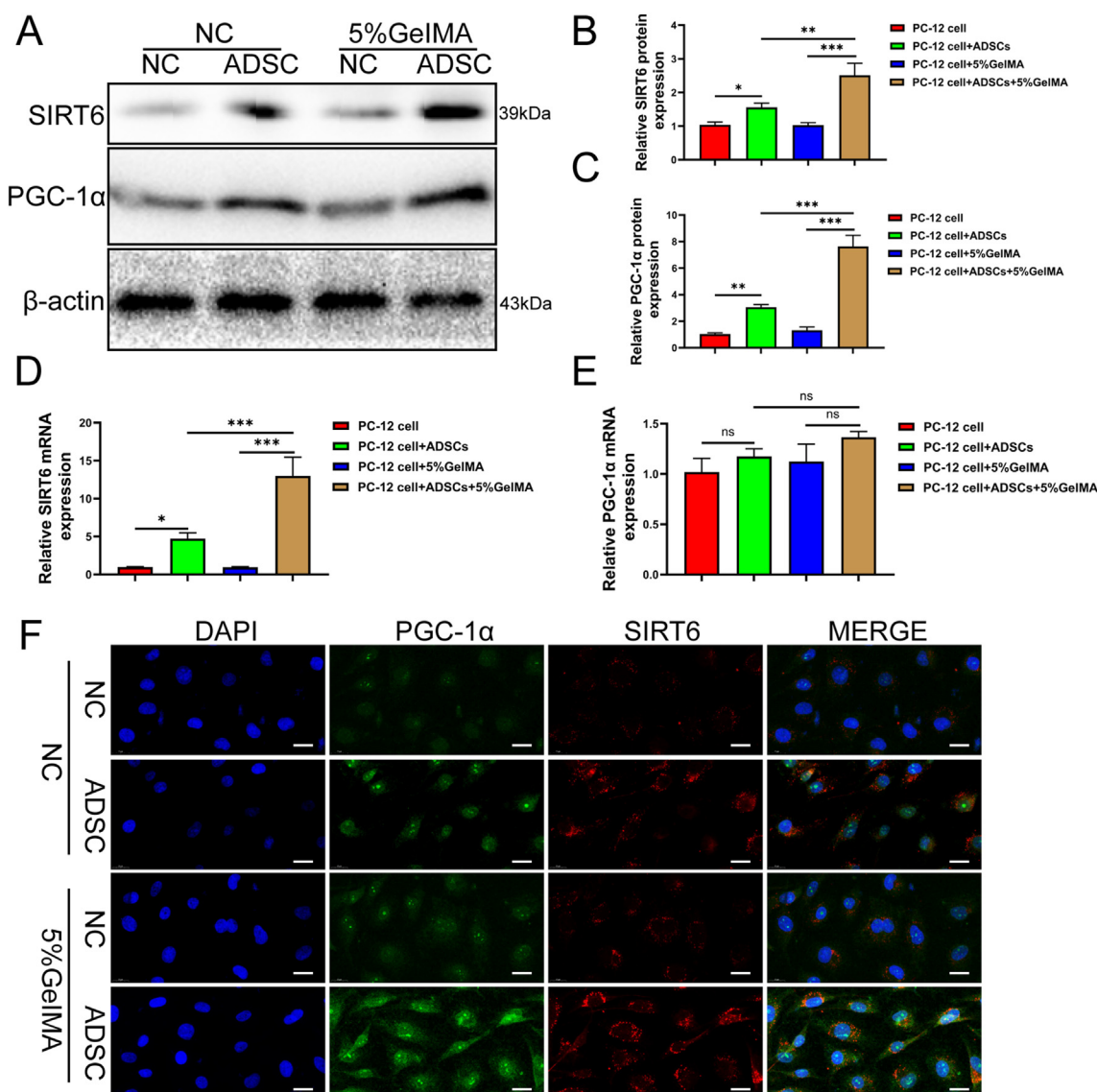
Fig. 4. ADSCs encapsulated in 5% GelMA significantly promoted the expression of SIRT6 and PGC-1α and the entry of PGC-1α into the nucleus of PC-12 cells. (A) Western blot was used to detect the expression of SIRT6 and PGC-1α in PC-12 cells. (B−C) The quantitative analysis of SIRT6 and PGC-1α protein expression. (D−E) Realtime-PCR was used to detect the mRNA expression of SIRT6 and PGC-1α in PC-12 cells. (F) Immunofluorescence staining of PC-12 cells in a co-culture system.

catheter alone group, suggesting that the PLGA catheter + GelMA-encapsulating ADSCs significantly increased the number and function of nerve fibers. The function of SIRT6 and PGC-1α proteins in the PLGA catheter + GelMA-encapsulating ADSCs group were significantly better than those in the PLGA + catheter alone group. The expression of SIRT6 and PGC-1α in the PLGA catheter + GelMA-encapsulating ADSCs group was higher than that in the catheter alone group (Fig. 7E and F), indicating that the PLGA catheter + GelMA-encapsulating ADSCs enhanced the growth of nerve by promoting the expression of SIRT6/PGC-1α pathway in the nerve.

4. Discussion

Peripheral nerve injury represents a type of nerve tissue injury posing a significant threat to the human nervous system, potentially resulting in sensory and motor dysfunction and even disability [35−37]. While peripheral nerves exhibit a degree of self-repair capability following injury, their axon growth is intricately regulated by various factors, such as phenotype transformation of Schwann cells, immune cell infiltration, neurovascular regeneration and so on [38−40]. Regenerated axons only proliferate at a rate of 1 mm per day [41], a supply insufficient to meet the recovery demands of patients.

Currently, primary treatment modalities for peripheral nerve injury encompass surgical repair, autologous nerve transplantation, nerve catheter synthesis, stem cell transplantation, and exosome extraction [42,43]. Despite autologous nerve transplantation being a prevalent treatment approach, it is associated with drawbacks such as limited donor tissue, damage to functional nerves, and the possibility of neuroma formation [13,43−46]. SCs are ideal choices for cell therapy applications due to their regenerative and immunomodulatory functions [47], and in recent years, more and more studies have suggested that mesenchymal stem cell-based therapies are promising for the treatment of nerve repair [48−50]. Studies have shown that transplanted MSCs can differentiate into Schwann cells *in vivo*, providing the support and nutrients needed for axonal growth [51,52]. Sowa et al. found that transplanted MSCs
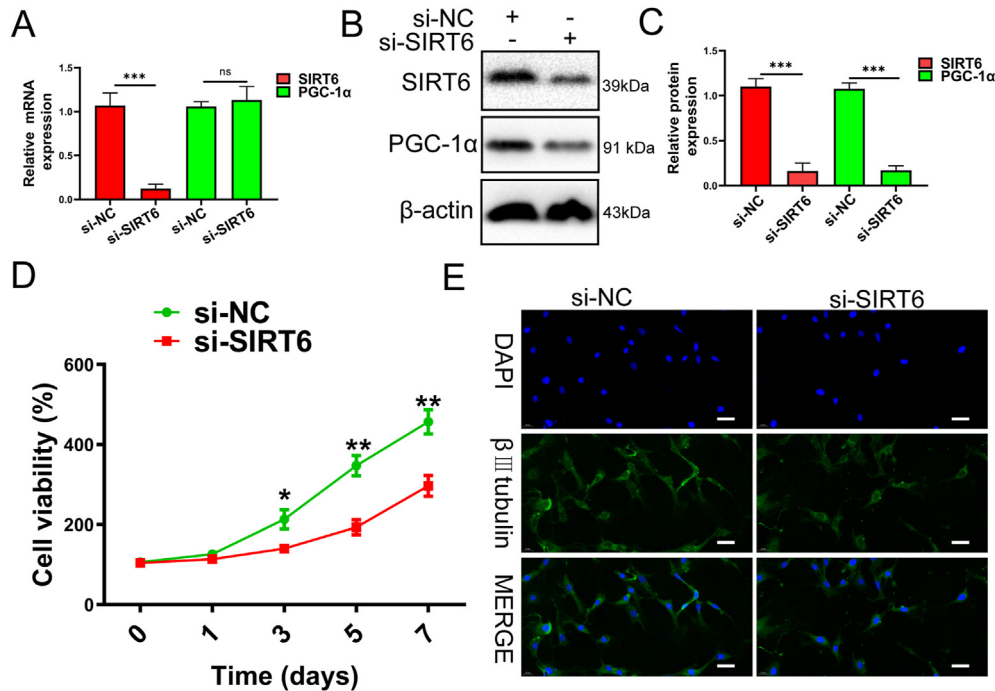
Fig. 5. Silencing of SIRT6 inhibits PC-12 differentiation levels. (A) Realtime-PCR was used to detect SIRT6 and PGC-1α mRNA expression of PC-12 cells. (B) Western blot was used to detect the protein expression levels of SIRT6 and PGC-1α. (C) Histograms of quantitative analysis of SIRT6 and PGC-1α protein expression. (D) CCK-8 detects PC-12 activity. (E) Immunofluorescence staining of PC-12 cells.
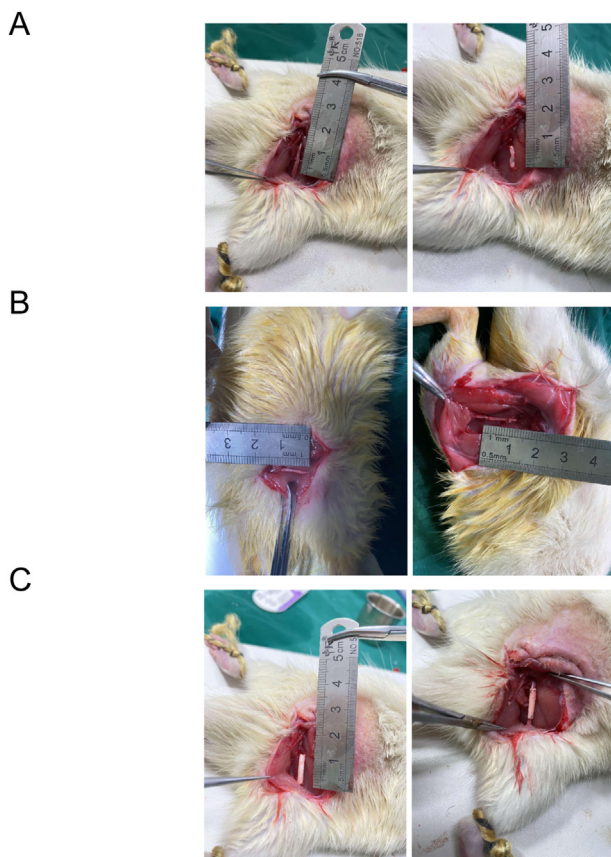

Fig. 6. The process of peripheral nerve injury model construction. (A) The right sciatic nerve of rat was exposed, and a 10 mm long section of nerve tissue was cut off. (B) The nerve was inverted 180° and sutured back in situ. (C) Prepare a 12 mm PLGA catheter and suture the two severed ends of the nerve with the PLGA catheter sleeve.

had a positive effect on axon outgrowth, myelin formation, and the recovery of denervated muscle atrophy [53]. ADSCs are widely distributed, low immunogenic, and anti-fibrotic, and are widely used in the treatment of diseases [54]. Indeed, there are many ways to transplant stem cells, such as microinjection, but this method may damage stem cells and delicate intraneural structures, resulting in abnormal cell distribution [51]. GelMA has the effect of enhancing cell binding, promoting cell viability and proliferation. Therefore, we used GelMA to encapsulate ADSCs for the experiment.

The cellular activity of ADSCs encapsulated in 5% GeIMA and 10% GeIMA by CCK-8 and ELISA respectively and the results demonstrated an increased cellular activity of ADSCs and the promoted protein levels of BDNF, GDNF, and β-NGF of ADSCs. The results showed that the protein levels of BDNF, GDNF and β-NGF in 5% GeIMA were higher than those in 10% GeIMA. 5% GeIMA has more space, while 10% GeIMA inhibits the growth of ADSCs. Subsequently, PC-12 cells were employed for four group, specifically PC-12 cells cultured alone, PC-12 cells + ADSCs, PC-12 cells + 5% GeIMA, and PC-12 cells + 5% GeIMA + encapsulated ADSCs. Our findings demonstrated that the mRNA expression levels of BDNF, GDNF, and β-NGF were most pronounced when ADSCs encapsulated in 5% GeIMA co-cultured with PC-12 cells. 5% substrate better supports ADSCs activity. There might be two reasons for this. Firstly, compared to 5%, 10% restricted the range of cell growth, the cell could not be fully stretched, and the cell function was impaired. Secondly, the higher percentage of gel causes that the active factors are not so easily released to the media and they stay trapped inside.

According to Zou et al., inhibition of SIRT6 inhibits macrophage migration, phagocytosis, and M2 polarization, delaying peripheral nerve recovery [32]. PGC-1α is a group involved in neuronal metabolism, neurotransmission, and morphological genesis [33]. Next, we experimentally verified the role of SIRT6/PGC-1α pathway in PC-12 cells co-cultured with ADSCs encapsulated in 5% GeIMA.
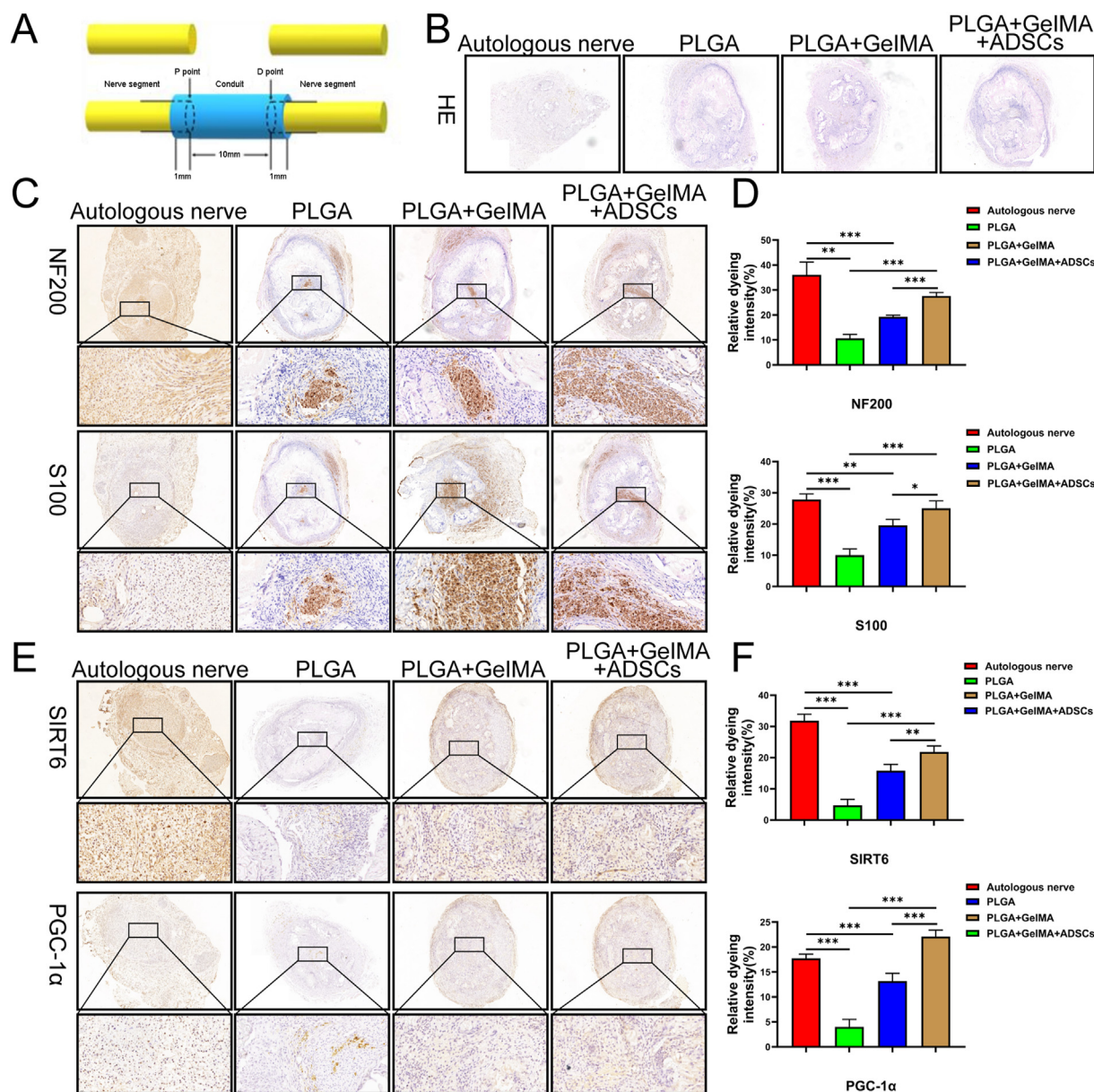
Fig. 7. ADSCs encapsulated in 5% GelMA markedly promoted the repair of sciatic nerve. (A) The Transplant schematic was shown. (B) HE staining shows neurological condition. (C) Immunohistochemical staining of NF200 and S100 expression. (D) Histogram of NF200 and S100 expression quantification. (E) Expression of SIRT6 and PGC-1α by immuno-histochemical staining. (F) Histogram of SIRT6 and PGC-1α expression quantification. ***$p < 0.001$, **$p < 0.01$, *$p < 0.05$ (n = 5).

Western blot experiments showed that the expression levels of SIRT6 and PGC-1α were higher in PC-12 cells + ADSCs encapsulated in 5% GelMA than PC-12 cells + ADSCs. These results showed that co-culture with ADSCs encapsulated in 5% GelMA promoted the expression of SIRT6 and PGC-1α compared with co-culture with ADSCs alone. However, Realtime-PCR results showed that there was no significant change in PGC-1α mRNA expression. We then silenced SIRT6 in PC-12 cells, and Realtime-PCR showed that mRNA expression levels of PGC-1α remained largely unchanged, but PGC-1α protein expression levels decreased significantly. Western blot results showed that the protein levels of SIRT6 and PGC-1α decreased significantly after silencing SIRT6, indicating that silencing of SIRT6 significantly inhibited the protein expression level of PGC-1α rather than mRNA level. CCK-8 results revealed a significant reduction in PC-12 cell activity. The results from immunofluorescence indicated a concurrent inhibition of PC-12 cell

differentiation. These results showed that silencing of SIRT6 restrained the extent of PC-12 cell differentiation. Finally, immunohistochemical experiments were conducted on autologous nerves, common PLGA catheters, PLGA catheters + 5% GelMA, and PLGA catheters + ADSCs encapsulated in 5% GelMA, confirming our hypothesis regarding the significant enhancement of nerve fibers number and functionality as a result of PLGA catheters filled with ADSCs encapsulated in 5% GelMA.

Notably, the expression of SIRT2, PGC-1α, NF200 and S100 were significantly elevated in PLGA catheters filled with ADSCs encapsulated in 5% GelMA compared to that in the PLGA catheter alone group and PLGA + 5% GelMA group. The quantity of nerves was also heightened in PLGA catheters filled with ADSCs encapsulated in 5% GelMA. These results suggested that PLGA catheters, when infused with 5% GelMA-encapsulated ADSCs, possesses the characteristics required for an ideal catheter *in vivo*.

Our study had some limitations. Firstly, we know that multiple neurotrophic factors, including nerve growth factor (NGF) and glial-cell-derived neurotrophic factors (GDNFs), promote axon outgrowth [55]. The exosomes functions as a natural carrier system for intercellular communication, facilitating the transfer of critical genetic information such as mRNA, proteins, and lipids between donor and recipient cells, and exhibiting regulatory effects on a diverse array of physiological and pathological processes *in vivo* [54—56]. The work of Bucan et al. suggested the presence of growth factors such as BDNF, GDNF, and NGF in ADSCs exosomes [43]. We speculated that ADSCs encapsulated in 5% GeIMA might secrete more exosomes than ADSCs without encapsulation of 5% GeIMA, and transmit nerve growth factors, genetic materials, and proteins to culture medium through exosomes. Secondly, SIRT6 has an impact on protein level through a variety of enzymatic activities, including deacetylation, fatty acylation, and ADP ribosylation [57—61]. These activities allow SIRT6 to modulate PGC-1α expression levels in a variety of ways. NAD + -dependent histone deacetylase is the most significant feature of SIRT6 [58,62], but we found no significant changes in mRNA expression levels of PGC-1α. Therefore, we hypothesized that SIRT6 regulated the expression level of PGC-1α protein through other pathways such as ubiquitinase, deubiquitinase, lactinase, etc. These limitations needed to be further experimentally proven.

5. Conclusion

In this study, we constructed a 3D co-culture model by co-culturing ADSCs, PC-12 cells and 5% GeIMA, and verified that the activity of ADSCs could be promoted with 5% GeIMA, and the effect of 5% GeIMA was better than that of 10% GeIMA. We found that the co-culture system promoted the secretion of BDNF, GDNF, and β-NGF, and promoted the differentiation of PC-12 cells. We further explored the mechanism of co-culture system, studied the role of SIRT6 and PGC-1α and confirmed that SIRT6 promoted the differentiation of PC-12 cells by regulating the level of PGC-1α protein, which was of great significance in the field of peripheral nerve repair.

Fundings

Data availability statement

All data that support the findings of this study can be requested from the correspondent authors for reasonable reasons.

Declaration of competing interest

The authors declare that they have no known competing financial interests or personal relationships that could have appeared to influence the work reported in this paper.

References

[1] Lim EF, Nakanishi ST, Hoghooghi V, Eaton SE, Palmer AL, Frederick A, et al. AlphaB-crystallin regulates remyelination after peripheral nerve injury. Proc Natl Acad Sci U S A 2017;114(9):E1707. e16.

[2] Li R, Liu Z, Pan Y, Chen L, Zhang Z, Lu L. Peripheral nerve injuries treatment: a systematic review. Cell Biochem Biophys 2014;68(3):449—54.

[3] Scheib J, Höke A. Advances in peripheral nerve regeneration. Nat Rev Neurol 2013;9(12):668—76.

[4] Raza C, Riaz HA, Anjum R, Shakeel NUA. Repair strategies for injured peripheral nerve: review. Life Sci 2020;243:117308.

[5] Daly W, Yao L, Zeugolis D, Windebank A, Pandit A. A biomaterials approach to peripheral nerve regeneration: bridging the peripheral nerve gap and enhancing functional recovery. J R Soc Interface 2012;9(67):202—21.

[6] Grinsell D, Keating CP. Peripheral nerve reconstruction after injury: a review of clinical and experimental therapies. BioMed Res Int 2014;2014:698256.

[7] Muheremu A, Ao Q. Past, present, and future of nerve conduits in the treatment of peripheral nerve injury. BioMed Res Int 2015;2015:237507.

[8] Cattin AL, Burden JJ, Van Emmenis L, Mackenzie FE, Hoving JJ, Garcia Calavia N, et al. Macrophage-Induced blood vessels guide Schwann cell-mediated regeneration of peripheral nerves. Cell 2015;162(5):1127—39.

[9] Liu S, Yang H, Chen D, Xie Y, Tai C, Wang L, et al. Three-dimensional bio-printing sodium alginate/gelatin scaffold combined with neural stem cells and oligodendrocytes markedly promoting nerve regeneration after spinal cord injury. Regenerative biomaterials 2022;9:rbac038.

[10] Lategan M, Kumar P, Choonara YE. Functionalizing nanofibrous platforms for neural tissue engineering applications. Drug Discov Today 2022;27(5): 1381—403.

[11] Tang X, Li Q, Huang T, Zhang H, Chen X, Ling J, et al. Regenerative role of T cells in nerve repair and functional recovery. Front Immunol 2022;13:923152.

[12] Rhode SC, Beier JP, Ruhl T. Adipose tissue stem cells in peripheral nerve regeneration-In vitro and in vivo. J Neurosci Res 2021;99(2):545—60.

[13] Kingham PJ, Kalbermatten DF, Mahay D, Armstrong SJ, Wiberg M, Terenghi G. Adipose-derived stem cells differentiate into a Schwann cell phenotype and promote neurite outgrowth in vitro. Exp Neurol 2007;207(2):267—74.

[14] Li X, Ding J, Zhang Z, Yang M, Yu J, Wang J, et al. Kartogenin-incorporated thermogel supports stem cells for significant cartilage regeneration. ACS Appl Mater Interfaces 2016;8(8):5148—59.

[15] Eren F, Öksüz S, Küçükodaci Z, Kendırlı MT, Cesur C, Alarçın E, et al. Targeted mesenchymal stem cell and vascular endothelial growth factor strategies for repair of nerve defects with nerve tissue implanted autogenous vein graft conduits. Microsurgery 2016;36(7):578—85.

[16] Zhang P, He X, Liu K, Zhao F, Fu Z, Zhang D, et al. Bone marrow stromal cells differentiated into functional Schwann cells in injured rats sciatic nerve. Artif Cells Blood Substit Immobil Biotechnol 2004;32(4):509—18.

[17] Zheng Y, Huang C, Liu F, Lin H, Niu Y, Yang X, et al. Reactivation of denervated Schwann cells by neurons induced from bone marrow-derived mesenchymal stem cells. Brain Res Bull 2018;139:211—23.

[18] Fu X, Tong Z, Li Q, Niu Q, Zhang Z, Tong X, et al. Induction of adipose-derived stem cells into Schwann-like cells and observation of Schwann-like cell proliferation. Mol Med Rep 2016;14(2):1187—93.

[19] El-Badawy A, Amer M, Abdelbaset R, Sherif SN, Abo-Elela M, Ghallab YH, et al. Adipose stem cells display higher regenerative capacities and more adaptable electro-kinetic properties compared to bone marrow-derived mesenchymal stromal cells. Sci Rep 2016;6:37801.

[20] Qu J, Zhang H. Roles of mesenchymal stem cells in spinal cord injury. Stem Cell Int 2017;2017:5251313.

[21] Yin J, Yan M, Wang Y, Fu J, Suo H. 3D bioprinting of low-concentration cell-laden gelatin methacrylate (GelMA) bioinks with a two-step cross-linking strategy. ACS Appl Mater Interfaces 2018;10(8):6849—57.

[22] Zhang Y, Chen H, Li J. Recent advances on gelatin methacrylate hydrogels with controlled microstructures for tissue engineering. Int J Biol Macromol 2022;221:91—107.

[23] Li Y, Liu D, Tan F, Yin W, Li Z. Umbilical cord derived mesenchymal stem cell-GelMA microspheres for accelerated wound healing. Biomed Mater (Bristol, U K) 2022;18(1).

[24] Huang Y, Xu K, Liu J, Dai G, Yin J, Wei P. Promotion of adrenal pheochromocytoma (PC-12) cell proliferation and outgrowth using Schwann cell-laden gelatin methacrylate substrate. Gels (Basel, Switzerland) 2022;8(2).

[25] Imai S, Armstrong CM, Kaeberlein M, Guarente L. Transcriptional silencing and longevity protein Sir 2 is an NAD-dependent histone deacetylase. Nature 2000;403(6771):795—800.

[26] Klar AJ, Strathern JN, Broach JR, Hicks JB. Regulation of transcription in expressed and unexpressed mating type cassettes of yeast. Nature 1981;289(5795):239—44.

[27] Frye RA. Characterization of five human cDNAs with homology to the yeast SIR2 gene: Sir2-like proteins (sirtuins) metabolize NAD and may have protein ADP-ribosyltransferase activity. Biochem Biophys Res Commun 1999;260(1): 273—9.

[28] Frye RA. Phylogenetic classification of prokaryotic and eukaryotic Sir2-like proteins. Biochem Biophys Res Commun 2000;273(2):793—8.

[29] Finkel T, Deng CX, Mostoslavsky R. Recent progress in the biology and physiology of sirtuins. Nature 2009;460(7255):587—91.

[30] Kugel S, Mostoslavsky R. Chromatin and beyond: the multitasking roles for SIRT6. Trends Biochem Sci 2014;39(2):72—81.

[31] Rodgers JT, Puigserver P. Certainly can't live without this: SIRT6. Cell Metabol 2006;3(2):77—8.

[32] Zou Y, Zhang J, Xu J, Fu L, Xu Y, Wang X, et al. SIRT6 inhibition delays peripheral nerve recovery by suppressing migration, phagocytosis and M2-polarization of macrophages. Cell Biosci 2021;11(1):210.

[33] McMeekin LJ, Bartley AF, Bohannon AS, Adlaf EW, van Groen T, Boas SM, et al. A role for PGC-1α in transcription and excitability of neocortical and hippocampal excitatory neurons. Neuroscience 2020;435:73—94.

[34] Zhou H, Liu S, Zhang N, Fang K, Zong J, An Y, et al. Downregulation of Sirt6 by CD38 promotes cell senescence and aging. Aging 2022;14(23):9730—57.

[35] Dong R, Liu Y, Yang Y, Wang H, Xu Y, Zhang Z. MSC-derived exosomes-based therapy for peripheral nerve injury: a novel therapeutic strategy. BioMed Res Int 2019;2019:6458237.

[36] Panagopoulos GN, Megaloikonomos PD, Mavrogenis AF. The present and future for peripheral nerve regeneration. Orthopedics 2017;40(1):e141–56.

[37] Zack-Williams SD, Butler PE, Kalaskar DM. Current progress in use of adipose derived stem cells in peripheral nerve regeneration. World J Stem Cell 2015;7(1):51–64.

[38] Zhang H, Shao Z, Zhu Y, Shi L, Li Z, Hou R, et al. Toll-like receptor 4 (TLR4) expression affects Schwann cell behavior in vitro. Sci Rep 2018;8(1):11179.

[39] Caillaud M, Richard L, Vallat JM, Desmoulière A, Billet F. Peripheral nerve regeneration and intraneural revascularization. Neural regeneration research 2019;14(1):24–33.

[40] Chen P, Piao X, Bonaldo P. Role of macrophages in Wallerian degeneration and axonal regeneration after peripheral nerve injury. Acta Neuropathol 2015;130(5):605–18.

[41] Seddon HJ, Medawar PB, Smith H. Rate of regeneration of peripheral nerves in man. J Physiol 1943;102(2):191–215.

[42] Li X, Guan Y, Li C, Zhang T, Meng F, Zhang J, et al. Immunomodulatory effects of mesenchymal stem cells in peripheral nerve injury. Stem Cell Res Ther 2022;13(1):18.

[43] Bucan V, Vaslaitis D, Peck CT, Strauß S, Vogt PM, Radtke C. Effect of exosomes from rat adipose-derived mesenchymal stem cells on neurite outgrowth and sciatic nerve regeneration after crush injury. Mol Neurobiol 2019;56(3):1812–24.

[44] Chalfoun CT, Wirth GA, Evans GR. Tissue engineered nerve constructs: where do we stand? J Cell Mol Med 2006;10(2):309–17.

[45] Hu J, Zhu QT, Liu XL, Xu YB, Zhu JK. Repair of extended peripheral nerve lesions in rhesus monkeys using acellular allogenic nerve grafts implanted with autologous mesenchymal stem cells. Exp Neurol 2007;204(2):658–66.

[46] Marchesi C, Pluderi M, Colleoni F, Belicchi M, Meregalli M, Farini A, et al. Skin-derived stem cells transplanted into resorbable guides provide functional nerve regeneration after sciatic nerve resection. Glia 2007;55(4):425–38.

[47] Naserian S, Shamdani S, Arouche N, Uzan G. Regulatory T cell induction by mesenchymal stem cells depends on the expression of TNFR2 by T cells. Stem Cell Res Ther 2020;11(1):534.

[48] Mundra V, Gerling IC, Mahato RI. Mesenchymal stem cell-based therapy. Mol Pharm 2013;10(1):77–89.

[49] Ozawa K, Sato K, Oh I, Ozaki K, Uchibori R, Obara Y, et al. Cell and gene therapy using mesenchymal stem cells (MSCs). J Autoimmun 2008;30(3):121–7.

[50] di Summa PG, Kingham PJ, Raffoul W, Wiberg M, Terenghi G, Kalbermatten DF. Adipose-derived stem cells enhance peripheral nerve regeneration. J Plast Reconstr Aesthetic Surg : JPRAS 2010;63(9):1544–52.

[51] Jiang L, Jones S, Jia X. Stem cell transplantation for peripheral nerve regeneration: current options and opportunities. Int J Mol Sci 2017;18(1).

[52] Sullivan R, Dailey T, Duncan K, Abel N, Borlongan CV. Peripheral nerve injury: stem cell therapy and peripheral nerve transfer. Int J Mol Sci 2016;17(12).

[53] Sowa Y, Kishida T, Imura T, Numajiri T, Nishino K, Tabata Y, et al. Adipose-derived stem cells promote peripheral nerve regeneration in vivo without differentiation into schwann-like lineage. Plast Reconstr Surg 2016;137(2):318e–30e.

[54] Zhou Y, Yuan J, Zhou B, Lee AJ, Lee AJ, Ghawji Jr M, et al. The therapeutic efficacy of human adipose tissue-derived mesenchymal stem cells on experimental autoimmune hearing loss in mice. Immunology 2011;133(1):133–40.

[55] Kubo T, Randolph MA, Gröger A, Winograd JM. Embryonic stem cell-derived motor neurons form neuromuscular junctions in vitro and enhance motor functional recovery in vivo. Plast Reconstr Surg 2009;123(2 Suppl):139s–48s.

[56] György B, Szabó TG, Pásztói M, Pál Z, Misják P, Aradi B, et al. Membrane vesicles, current state-of-the-art: emerging role of extracellular vesicles. Cell Mol Life Sci : CMLS 2011;68(16):2667–88.

[57] Wang Y, Liu T, Cai Y, Liu W, Guo J. SIRT6's function in controlling the metabolism of lipids and glucose in diabetic nephropathy. Front Endocrinol 2023;14:1244705.

[58] Cantó C, Houtkooper RH, Pirinen E, Youn DY, Oosterveer MH, Cen Y, et al. The NAD(+) precursor nicotinamide riboside enhances oxidative metabolism and protects against high-fat diet-induced obesity. Cell Metabol 2012;15(6):838–47.

[59] Cheng J, Keuthan CJ, Esumi N. The many faces of SIRT6 in the retina and retinal pigment epithelium. Front Cell Dev Biol 2023;11:1244765.

[60] Wu K, Wang Y, Liu R, Wang H, Rui T. The role of mammalian Sirtuin 6 in cardiovascular diseases and diabetes mellitus. Front Physiol 2023;14:1207133.

[61] You Y, Liang W. SIRT1 and SIRT6: the role in aging-related diseases. Biochim Biophys Acta, Mol Basis Dis 2023;1869(7):166815.

[62] Wei W, Li T, Chen J, Fan Z, Gao F, Yu Z, et al. SIRT3/6: an amazing challenge and opportunity in the fight against fibrosis and aging. Cell Mol Life Sci : CMLS 2024;81(1):69.